Differential altered stability and transcriptional activity of ΔNp63 mutants in distinct ectodermal dysplasias

Gareth Browne[1], Rita Cipollone[2], Anna Maria Lena[2], Valeria Serra[2], Huiqing Zhou[3], Hans van Bokhoven[3], Volker Dötsch[4], Daniele Merico[5], Roberto Mantovani[5], Alessandro Terrinoni[2], Richard A. Knight[1], Eleonora Candi[2] and Gerry Melino[1,2,*]

[1]Medical Research Council, Toxicology Unit, Leicester University, Leicester LE1 9HN, UK
[2]Biochemistry Laboratory, IDI-IRCCS, c/o University of Rome 'Tor Vergata', 00133 Rome, Italy
[3]Department of Human Genetics, Nijmegen Centre for Molecular Life Sciences, Radboud University Nijmegen Medical Centre, 6500 HB Nijmegen, The Netherlands
[4]Institute of Biophysical Chemistry, Goethe University of Frankfurt, 60438 Frankfurt am Main, Germany
[5]Department of Biomolecular Science and Biotechnology, University of Milan, 20133 Milan, Italy
*Author for correspondence (gerry.melino@uniroma2.it)

Summary

Heterozygous mutations of p63, a key transcription factor in epithelial development, are causative in a variety of human ectodermal dysplasia disorders. Although the mutation spectrum of these disorders displays a striking genotype–phenotype association, the molecular basis for this association is only superficially known. Here, we characterize the transcriptional activity and protein stability of ΔNp63 mutants (that is, mutants of a p63 isoform that lacks the N-terminal transactivation domain) that are found in ectrodactyly–ectodermal dysplasia–cleft syndrome (EEC), ankyloblepharon–ectodermal dysplasia–clefting syndrome (AEC) and nonsyndromic split-hand/split-foot malformation (SHFM). DNA-binding and sterile alpha motif (SAM) domain mutants accumulate in the skin of EEC and AEC syndrome patients, respectively, and show extended half lives in vitro. By contrast, C-terminal mutations found in SHFM patients have half-lives similar to that of the wild-type protein. The increased half-life of EEC and AEC mutant proteins was reverted by overexpression of wild-type ΔNp63. Interestingly, the mutant proteins exhibit normal binding to and degradation by the E3 ubiquitin ligase Itch. Finally, EEC and AEC mutant proteins have reduced transcriptional activity on several skin-specific gene promoters, whereas SHFM mutant proteins are transcriptionally active. Our results, therefore, provide evidence for a regulatory feedback mechanism for p63 that links transcriptional activity to regulation of protein homeostasis by an unknown mechanism. Disruption of this regulatory mechanism might contribute to the pathology of p63-related developmental disorders.

Key words: p63, Skin, Ectodermal dysplasia protein, Stability, Itch

Introduction

p63 (Yang et al., 1998), a member of the p53 family, has an important role in development, and plays a vital role in regulating epithelial formation and in maintaining the proliferative capacity of epithelial stem cells (Candi et al., 2007b; Senoo et al., 2007). p63 is expressed as at least six different isoforms. Transcription from two different promoters, one preceding the first exon and a second within the third intron, give rise to either a transactivation domain containing (TA) or transactivation domain lacking (ΔN) N-termini of p63 (Yang et al., 1998). Alternative splicing of the C-terminus generates additional α-, β- and γ-isoforms, of which only the full length α-isoform contains the sterile alpha motif (SAM), thought to mediate protein–protein interactions (Cicero et al., 2006; Yang et al., 1998), and a transactivation inhibitory (TI) domain that can interact with the TA domain. This interaction consequently masks the residues that are important for transactivation, thereby suppressing TAp63-mediated transactivation (Serber et al., 2002; Yang et al., 1998). Interestingly, the ΔNp63 isoforms appear to contain a second transactivation domain (TA2) (Dohn et al., 2001; Duijf et al., 2002) and can therefore regulate expression of a distinct subset of genes as compared with the TAp63 isoforms (Candi et al., 2006). p63 function has been studied in animal models in which p63 expression was ablated (Mills et al., 1999; Yang et al., 1999)

or overexpressed (Candi et al., 2006). Knockout mice exhibit severe defects in limb, skin and craniofacial development, and die shortly after birth due to lack of an epidermal barrier (Gu et al., 2006; Laurikkala et al., 2006; Mills et al., 1999; Yang et al., 1999). In adult skin, ΔNp63α is by far the main isoform expressed in the basal layer of the epidermis (Candi et al., 2007a; Candi et al., 2007b; Yang et al., 1998). Although several p63 target genes have been identified (Carroll et al., 2006; Ellisen et al., 2002; Pozzi et al., 2009; Vigano et al., 2006; Yang et al., 2006), a complete assessment of p63 target genes activated in vivo is crucial to understanding of its function.

The expression of p63 has been found to be post-translationally regulated by the HECT-containing ubiquitin E3 ligase Itch (Rossi et al., 2006). Itch has been reported to bind via its WW domain to a PPxY consensus motif in p63, spanning residues 501–504 that lie immediately adjacent to the C-terminal SAM domain. More recently it has been shown that the expression of p63 is also under post-transcriptional regulation through the microRNA machinery by miR203 (Lena et al., 2008; Yi et al., 2008).

Ectodermal dysplasic syndromes (EDS) constitute a large group of autosomal dominant hereditary disorders of skin, orofacial and limb development that can be subdivided into a variety of individual syndromes according to their clinical manifestation (Rinne et al., 2006a). These syndromes include ectrodactyly–

ectodermal dysplasia–cleft lip/palate (EEC), ankyloblepharon–ectodermal dysplasia–clefting (AEC) and split-hand/split-foot malformation (SHFM). Heterozygous mutations in the *p63* gene have been found to be causative in a large proportion of human EDS (Rinne et al., 2007). An interesting feature of the involvement of p63 in EDS is that mutations associated with particular syndromes are clustered within specific domains of the p63 protein. Indeed, mutations causing the EEC syndrome are largely clustered within the DNA-binding domain (DBD), whereas mutations associated with AEC are largely confined to the SAM domain (Rinne et al., 2007). The C-terminal Q634X mutation is associated with SHFM, a disorder that does not have a skin phenotype.

It was initially thought that mutations within the DBD of p63 necessarily resulted in a dominant-negative loss of function by preventing DNA binding (Celli et al., 1999). However, this hypothesis has been confounded by the discovery that mutations in arginine 298 of the DBD, resulting in the EEC like syndromes Acro-Dermato-Ungual-Lacrimal-Tooth (ADULT) and limb mammary syndrome (LMS), produce a gain-of-function (Duijf et al., 2002; Rinne et al., 2006b). The molecular mechanism for the effect of mutations within the SAM and C-terminal domains of p63 are also unclear. Mutations within the SAM domain responsible for AEC syndrome were originally described as inhibiting the transactivation of a p53 consensus promoter by TAp63α, while also abolishing the ability of the ΔNp63α isoform to inhibit p53- or TAp63γ-mediated transactivation (McGrath et al., 2001). The L514F (leucine 514 to phenylalanine) mutation within the SAM domain has been demonstrated to impair the ability of ΔNp63α to bind and inhibit the splicing factors apobec-1-binding protein-1 (ABBP1) and SRA4, leading to aberrant spicing of components of the FGF and Notch signalling pathways and, indeed, of p63 itself (Candi et al., 2007b; Fomenkov et al., 2003; Huang et al., 2005). Mutations within the SAM domain of p63 have also been reported to prevent its direct binding and transcriptional regulation of the cell cycle checkpoint protein stratifin/14-3-3σ (Fomenkov et al., 2003; Westfall et al., 2003). The differential effect of mutations within different domains of p63 is underscored by recent reports on the transactivation of the *distalless* family members *Dlx3*, *Dlx5* and *Dlx6* by p63. Mutations in the SAM domain of p63 associated with AEC syndrome abolished the transactivation of *Dlx3* but not *Dlx5* and *Dlx6*; whereas mutations in the DBD domain abolished the transactivation of *Dlx5* and *Dlx6* (Lo Iacono et al., 2008; Radoja et al., 2007). More recently, it has been shown that p63 and IRF6 cooperate to prevent cleft palate in mice (Moretti et al., 2010; Thomason et al., 2010). Outstanding questions regarding the role of p63 mutation in EDS include: What is the role of the individual domains of p63? Why do mutations in a single gene give rise to phenotypically different diseases? What are the molecular mechanisms underlying these diseases?

Here, we examine the effect of disease-causing mutations within the DBD, SAM and C-terminal domains of the ΔNp63α isoform on its stability and ability to bind the ubiquitin E3 ligase Itch. We also examine the effect of p63 mutants on the ability to transactivate target genes known to be important in the development and maintenance of the stratified epithelium. Our results provide an initial understanding of the molecular mechanisms responsible for p63-related developmental disorders and suggest that defects in both transcription and degradation are involved in EDS pathogenesis.

Results

p63 accumulates in skin tissue of patients affected by EEC or AEC syndromes

We analyzed skin sections from normal individuals or patients using immunofluorescence and confocal analysis (Fig. 1A–C). In agreement with previous findings, nuclear p63 staining was
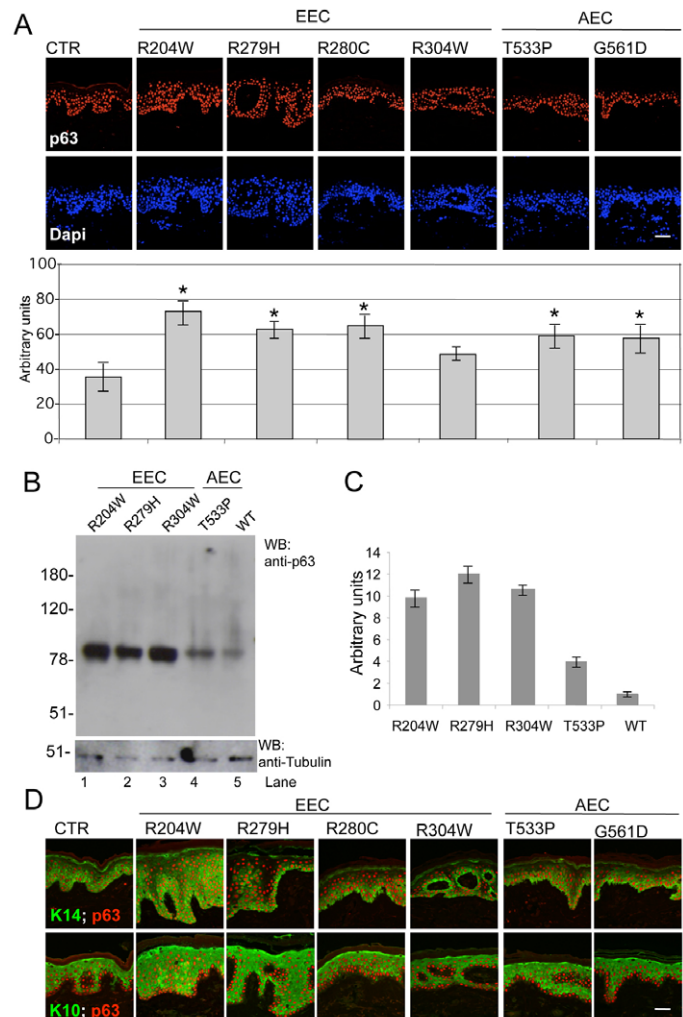
Fig. 1. Confocal analysis of p63 in skin tissue from a normal individual and from patients affected by EEC or AEC syndromes.
(**A**) Immunofluorescence detection of p63 (red) in normal and patient's skin. We analyzed three patients affected by EEC (R203W, R279H, R280 C, R304W) and two by AEC (T533P and G561D). Nuclear DNA content was visualised by DAPI staining (blue). Analysis of p63 expression was carried out using the software Nis Elements AR3.0 (Nikon) normalizing the intensity of the red staining versus nuclei number. Error bars were calculated by analyzing three sequential slides of each sample and indicate s.d. Statistical significance was evaluated by Student's *t*-test, 0.001<*P*<0.05. (**B**) Western blot analysis using protein extracts from patient cell lines indicate that DBD mutants significantly accumulated (about tenfold) in keratinocytes, whereas the SAM domain mutants analyzed accumulated to a lesser extent. (**C**) Quantification by densitometry is shown. (**D**) Confocal analysis of p63, K14, K10 and Ki67 in the skin tissue of a normal individual and from patients affected by EEC or AEC syndromes. Immunofluorescence detection of Ki67 (green, upper panel) shows no significant increase in proliferation in normal and patient's skin. K14, (green, middle panel) a basal layer maker, is expressed within normal levels as is K10 (green, lower panel), a spinous layer marker. Scale bars: 50 μm.

observed mainly in the basal keratinocyte layer and less in the spinous layer in normal controls. In patients affected by EEC (bearing the mutations R204W, R279H, R280C and R304W) and AEC (mutations T533P and G561D), p63 accumulates in basal and spinous layer keratinocytes as shown by increased red staining (Fig. 1A; quantification of the fluorescent signal is shown in the lower panel). To better evaluate p63 accumulation in the patient keratinocytes, we performed western blots using patient cell lines (Fig. 1B), and confirmed that the p63 protein strongly accumulates in patients affected by EEC (10- to 12-fold over controls; Fig. 1C) and, at a lower level, in a patient affected by AEC (fourfold over control; Fig. 1C). We next performed an immunohistochemical analysis of epidermal proliferation (keratin 14, K14) and differentiation (keratin 10, K10) markers. Most of these proteins, showed the expected staining patterns, both in control and patient skin (Fig. 1D). These results indicate that the p63 mutants accumulate in vivo in patients.

The effect of DBD, SAM and C-terminal domain mutation on steady-state stability and binding to Itch

To further study p63 mutant accumulation in patient tissue sections, we investigated 12 mutations in ΔNp63α known to give rise to phenotypically different ectodermal dysplasia-related syndromes. We chose the ΔNp63α isoform because it is by far the most highly expressed in the basal epithelium of developing limb buds and skin (Laurikkala et al., 2006). The mutations included six DBD mutations known to cause EEC syndrome, four SAM domain mutations known to cause AEC syndrome and one C-terminal domain mutation known to cause SHFM syndrome, along with two mutations of the lysine 637 residue in the C-terminal domain, which is known to be a target for sumoylation in TAp63α (Bakkers et al., 2005; Ghioni et al., 2005; Huang et al., 2004) (Fig. 2A). All the p63 mutations studied exhibited normal nuclear localization upon transfection in epithelial cell lines (supplementary material Fig. S1). We next examined the stability of wild-type and mutant ΔNp63α constructs 48 hours after overexpression in p53-null H1299 cells. Mutations within the DNA binding domain (Fig. 2B, lanes 2–7), and to a lesser extent in the SAM domain (Fig. 2B, lanes 8–11), resulted in increased expression as compared with the wild type; mutations within the C-terminal region had no observable effect (Fig. 2B). The increased expression could be due to an inability of these mutants to undergo ubiquitin-mediated degradation. To test this, we expressed them together with Itch, a ubiquitin E3 ligase known to target p63. Despite their higher basal expression levels, all mutants underwent Itch-mediated degradation as normal (Fig. 2C,D; lanes 4, 6, 8, 10, 12, 14). To further confirm that normal mutant degradation reflected their ability to interact with Itch, we carried out co-precipitation experiments with exogenously expressed enzymatically inactive Itch. We observed normal (supplementary material Fig. S2, lanes 9–12) or higher (supplementary material Fig. S2, lanes 3–8) interaction of the DBD and SAM mutants of p63 with Itch. Although there was no difference in the accumulation of the C-terminal domain mutants Q634X and K637Q, both also interacted normally with Itch (supplementary material Fig. S2, lanes 13, 14).

To confirm that the increased steady-state expression of the ΔNp63α DBD and SAM mutants was due an increased protein half-life, we exogenously expressed the mutants in H1299 cells and subjected them to [^{35}S]methionine pulse-chase followed by specific immunoprecipitation for metabolically labelled p63. Analysis of the time-course of exogenously expressed p63
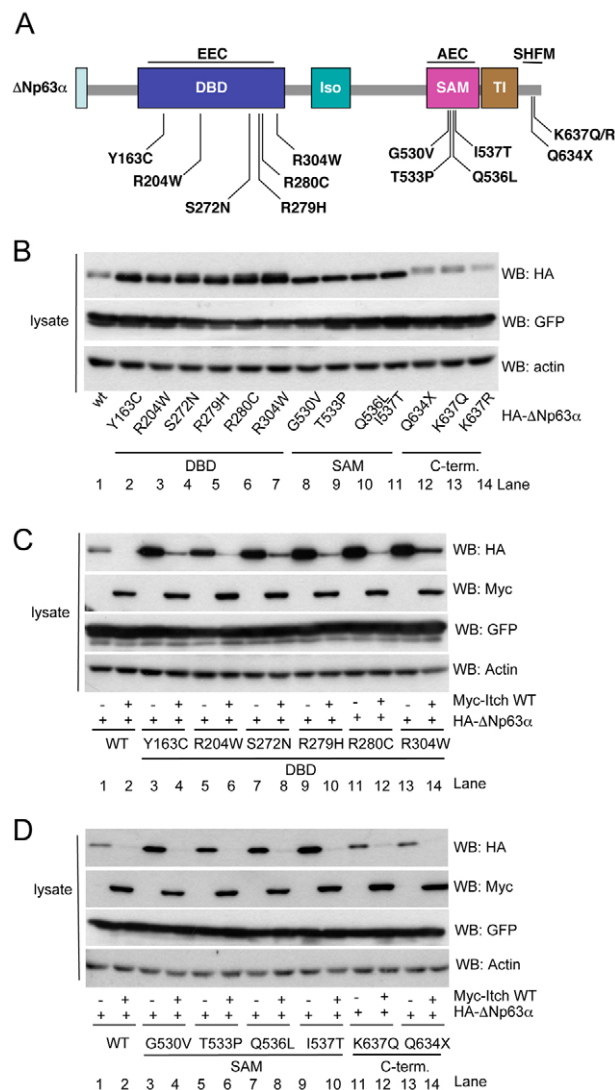
Fig. 2. Mutations of the DNA binding and SAM domains of ΔNp63α increase the steady-state protein stability without interfering with interaction with Itch. (**A**) Schematic diagram of ΔNp63α indicating the position of the DNA binding (DBD), isomerization (Iso), sterile alpha motif (SAM) and transactivation inhibitory (TI) domains. The location of the naturally occurring human mutations used in this study and the syndromes associated with them are indicated. Note that, for clarity, the positions of mutations in other p63 isoforms are indicated using the amino acid numbering system for TAp63α according to genetic classification reported in the literature (Rinne et al., 2007). (**B**) Mutants of the DBD or SAM but, not C-terminal domain, of ΔNp63α showed increased steady-state protein stability. H1299 cells were co-transfected with expression vectors for wild-type, DBD, SAM or C-terminal domain mutant HA-tagged ΔNp63α (HA-ΔNp63α). The panels show the input lysates probed with anti-HA and anti-actin antibodies. (**C**) Mutants of the DBD domain of ΔNp63α were degraded normally by Itch. H1299 cells were co-transfected with expression vectors for wild-type or DBD domain mutant HA-tagged ΔNp63α (HA-ΔNp63α), myc-tagged wild-type Itch (myc-Itch WT), and GFP vector as transfection control. The panels show the input lysates probed with anti-HA, anti-myc, anti-actin and anti-GPF antibodies. (**D**) Mutants of the SAM or TI domain of ΔNp63α were degraded normally by Itch. H1299 cells were co-transfected with expression vectors for wild-type, SAM or TI domain mutant HA-tagged ΔNp63α (HA-ΔNp63α), myc-tagged wild-type Itch (myc-Itch WT), and GFP vector as transfection control. The panels show the input lysates probed with anti-HA, anti-myc, anti-actin and anti-GFP antibodies. A representative experiment out of three is shown.

degradation in H1299 cells by [³⁵S]methionine pulse-chase revealed a greatly extended half-life for the DBD mutants of more than 6 hours (Fig. 3A,B) and a significantly extended half-life for the SAM domain mutants, from approximately 1.5 hours to 4.5 hours (Fig. 3C,D), consistent with the data in Fig. 1B.

We then investigated whether the coexpression of wild-type FLAG-tagged ΔNp63α would be able to reduce the expression of exogenously expressed DBD mutant (R280C) ΔNp63α. In Fig. 4A we show that coexpression of wild-type ΔNp63α did indeed reduce the expression of the mutant protein whereas coexpression of mutant R279H p63 was unable to achieve this (compare lanes 2 and 4 with lanes 2 and 6). This result suggests that wild-type, but not mutant, ΔNp63α might be involved in a feedback loop decreasing its own stability (compare lanes 1 and 3), perhaps by regulating an as-yet-unidentified ubiquitin E3 ligase. A further indication of this was provided when FLAG-tagged wild-type and DBD mutant ΔNp63α were exogenously expressed along with haemagglutinin (HA) tagged ubiquitin. The level of ubiquitylation of the wild-type protein was found to be higher than that of the mutant protein (Fig. 4B). To identify genes involved in this process, we performed transcriptional profiling analysis in SaOs-2 cells upon expression of ΔNp63 and, for comparison, TAp63. Enrichment analysis of Gene Ontology-derived gene sets identified a cluster of genes, corresponding to the 9.3% of the modulated genes (supplementary material Table S1) involved in ubiquitylation and protein degradation (Fig. 4). Interestingly, both ΔNp63 and TAp63 exerted a similar effect on the transcription of these ubiquitylation- and degradation-related genes. Three genes from this set, RNF144B, MDM2 and HERC4, were validated by real-time PCR (Fig. 4D).

Although we failed to identify a specific new degradation pathway involving ΔNp63, this data provides an indication that p63 target genes control p63 protein stability.

Effect of ΔNp63α mutations on skin-specific promoter transactivation

We next decided to examine the effect of EDS-related mutations of p63 on its ability to transactivate several promoters known to be important in skin development (Fig. 5). As a prelude to examining the ability of the DBD, SAM and C-terminal domain mutants of p63 to transactivate skin-specific promoters we decided to investigate both the ability of ΔNp63α mutants to bind DNA and its subcellular localization. In chromatin immunoprecipitation (ChIP) experiments using consensus p53 binding sites from the K14 promoter (Candi et al., 2006) (Fig. 5A), we confirmed that there was no alteration in the ability of the SAM domain mutants of ΔNp63α to bind DNA, whereas the DBD mutants analyzed had different binding capabilities. We also investigated the subcellular localization of the DBD, SAM and C-terminal domain mutants of ΔNp63α when exogenously expressed in H1299 cells. Confocal microscopy for ΔNp63α revealed normal nuclear localization for all the mutants examined (supplementary material Fig. S1), which confirmed that any alteration in transactivational capacity cannot be due to mislocalization of the exogenously expressed proteins.

To determine the transactivation capacity on skin-specific promoters, we transfected cells with either wild-type or EDS mutant ΔNp63α together with reporter constructs containing the luciferase gene under the control of the K14 promoter and the BPAG-1 promoter. Wild-type ΔNp63α was able to transactivate
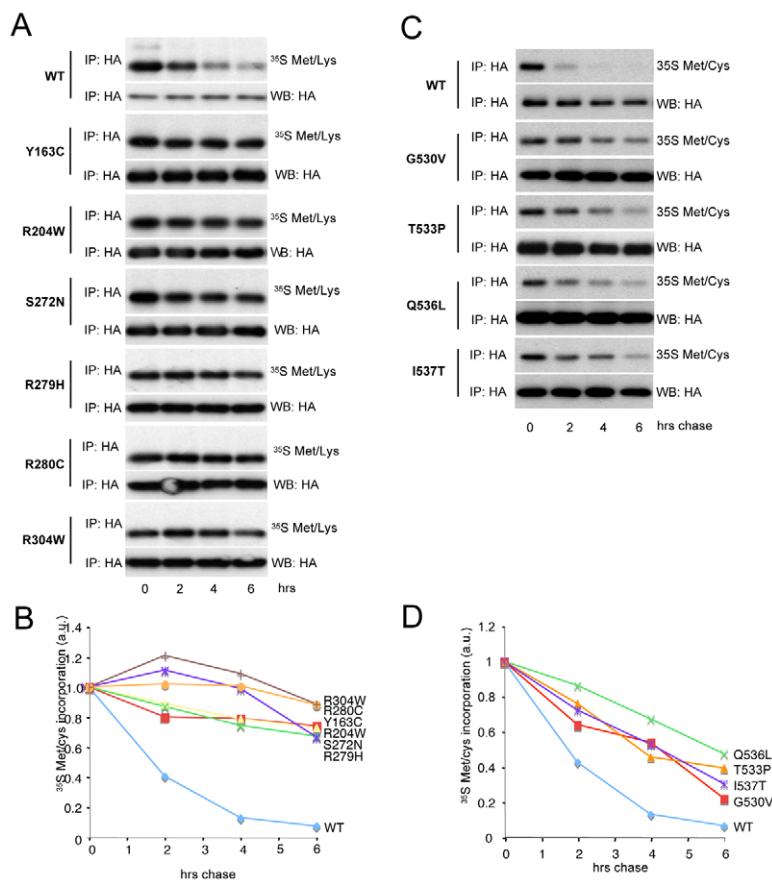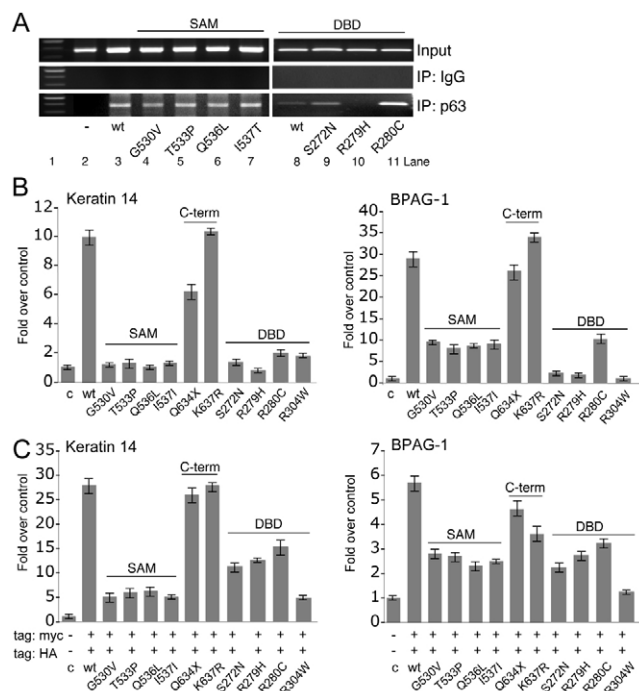

Fig. 3. ³⁵S pulse-chase reveals decreased degradation of DBD and SAM mutant ΔNp63α. H1299 cells were transfected with expression vectors for wild-type and DBD mutant (**A**) or SAM mutant (**C**) HA-tagged ΔNp63α and subjected to [³⁵S]methionine pulse-chase. Following immunoprecipitation, the bands detected by autoradiography and western blotting were quantified and the results normalized to incorporation at 0 hours and to total immunoprecipitated HA-tagged p63 protein. Autoradiography bands and immunological bands were quantified for DBD (**B**) or SAM (**D**) and results normalized to incorporation at time 0 and to total immunoprecipitated HA-tagged p63 protein. A representative experiment out of four is shown.
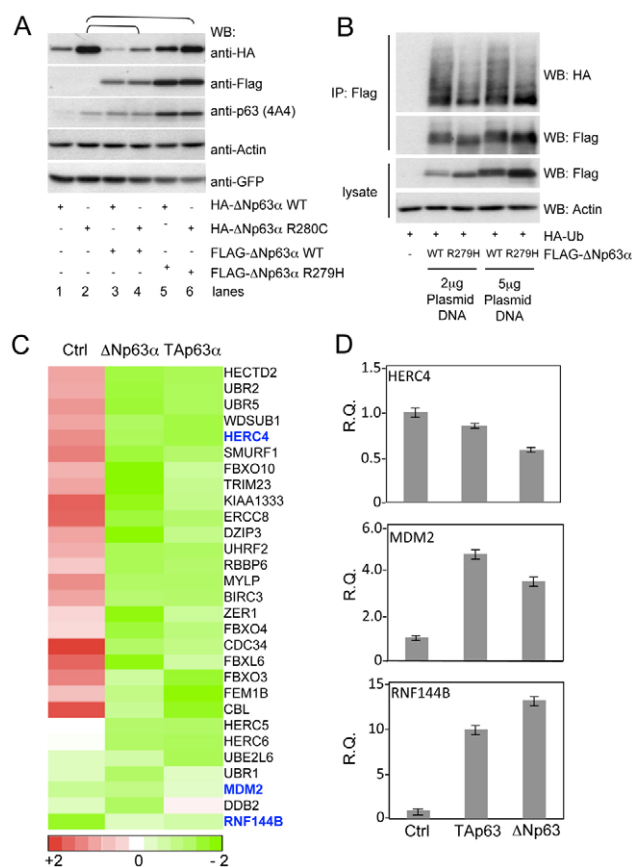
Fig. 4. The increased stability of DBD mutant ΔNp63α can be reversed by coexpression of excess wild-type ΔNp63α. (A) H1299 cells were co-transfected with 2.5 μg expression vectors for HA-tagged wild-type or DBD mutant ΔNp63α (HA-ΔNp63α) and 5 μg FLAG-tagged wild-type or DBD mutant ΔNp63α (FLAG-ΔNp63α) or empty pcDNA3-HA vector to normalize DNA levels and GFP. The panels show the cell lysates probed with anti-HA, anti-FLAG, anti-p63 (4A4 pan p63), anti-GFP and anti-actin antibodies. **(B)** Decreased ubiquitylation of DBD mutant ΔNp63α. H1299 cells were co-transfected with expression vectors for poly HA-tagged ubiquitin and 2 or 5 μg of FLAG-tagged wild-type or DBD mutant ΔNp63α. An anti-FLAG immunoprecipitation was carried out and the immunoprecipitate probed for FLAG-p63 and HA-ubiquitin. A representative experiment of three is shown. **(C)** Cluster of genes involved in ubiquitylation and protein degradation identified by enrichment analysis of Gene Ontology. Genes were found mainly downregulated, as indicated by the heat map presentation. **(D)** Validation of the gene array analysis by quantitative PCR. Real-time PCR analysis was performed to amplify the indicated transcripts using the same RNA samples that were used for the microarray assay. Bars show means ± s.d.

Fig. 5. Point mutations of ΔNp63α affect its transactivation activity on skin-specific promoters. (A) ChIP of p63 protein on the K14 promoter using oligonucleotides for the main p53-like binding site. ChIP was performed using nuclear extracts from untransfected and transfected HEK293 cell lines for the SAM domain mutants (G435V, T533P, Q536L, I537T) and the DBD mutants (S272N, R279H, R280C). A representative result of two independent experiments is shown. **(B,C)** Measurement of ΔNp63α mutant transactivation activity. (B) K14 and BPAG-1 promoters cloned in the luciferase reporter vector were used individually or co-transfected in HEK293 cells with an empty expression vector (pcDNA-HA) as control (c) or in cells expressing the indicated ΔNp63α proteins: wild-type (wt), SAM domain (G530V, T533P, Q536L, I537T), the C-terminal domain mutants (Q634X and K637R), and the DBD mutants (S272N, R279H, R280C, R304W). All luciferase assays were normalized for transfection efficiency with a *Renilla* reporter vector. (C) SAM and DBD domain mutants have dominant-negative effect on p63 transcriptional activity. K14 and BPAG-1 promoters cloned in the luciferase reporter vector were co-transfected in HEK293 cells with myc-tagged wild-type ΔNp63α and HA-tagged mutants p63: wild-type, SAM domain (G530V, T533P, I537T), the C-terminal domain mutants (Q634X and K637R), and the DBD mutants (S272N, R279H, R280C, R304W). All luciferase assays were normalized for transfection efficiency with a *Renilla* reporter vector. The results shown in B and C are representative of at least three independent experiments performed each time in triplicate, and error bars indicate s.d. Western blotting with HA-tag-specific and myc-tag-specific antibodies were performed to verify protein expression.

the two promoters (Fig. 5B). Both SAM and DBD mutations resulted in inhibition of the transactivational capability of ΔNp63α on the two promoters tested. The natural C-terminal domain mutant (Q634X) and K637R both enhanced K14 and BPAG-1 promoter activity. We next tested the effect of coexpressing wild-type and mutant ΔNp63α on skin promoter transactivation. SAM and DBD mutants were able to suppress the transactivation of both K14 and BPAG-1 promoters by the wild-type protein, whereas the C-terminal mutants had no inhibitory effects (Fig. 5C). To further examine the transcriptional activity of the mutant Q634X and to extend the observation described in Fig. 5, we performed quantitative real-time PCR upon expression of exogenous wild-type and mutated ΔNp63 in cells to evaluate the transcript levels of several p63 target genes. Interestingly, we found that the mutant Q634X had different effects on p63 transcriptional activity in comparison with the wild type: it displayed increased activity towards the targets PERP and Cyc D1, decreased activity towards DSP, PROX1, DLL1, MTUS1 and K17, and had unchanged activity towards p21.

Discussion

In this study, we have investigated the phenotype–genotype relationship between EDS and mutations in ΔNp63α. The data
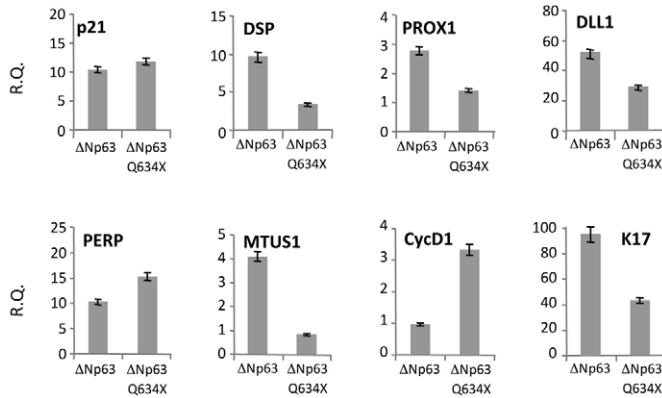
Fig. 6. Expression analysis of the target genes: comparison between wild-type ΔNp63 and Q634X mutant. Real-time PCR of the indicated target genes with RNA extracted from transfected HEK293 cells. Efficiencies of transfection were compared by GFP co-transfection. The results shown are average of three independent experiments ± s.d.

show that mutations in the DBD and SAM domains are associated with EEC and AEC, which have a skin phenotype, whereas mutations in the C-terminus cause SHFM, which does not. The DBD and SAM mutants, but not those in the C-terminus, result in increased protein stability, as shown by their enhanced expression in the skin of affected patients and by in vitro studies. Moreover, DBD and SAM mutations, but, again, not those in the C-terminus, result in reduced transcriptional activity on skin-specific promoters (Fig. 5D).

The increased stability of the DBD and SAM mutants is difficult to explain. All the mutants tested bind efficiently to the E3 ubiquitin ligase, Itch, which we have shown to be important for the proteasomal degradation of ΔNp63α. At least the R279H DBD mutant can be ubiquitylated, albeit less efficiently than the wild-type protein (Fig. 4B). Coexpression of wild-type ΔNp63α with a DBD domain mutant resulted in increased degradation of the mutant protein (Fig. 4A), suggesting that wild-type ΔNp63α is able to induce factors that augment ubiquitin-dependent or ubiquitin-independent mutant degradation. Indeed, merely increasing wild-type ΔNp63α expression also seems to destabilize

the wild-type protein. The R280C DBD mutant, however, is unable to increase R279H degradation. Indeed, the enrichment analysis of Gene Ontology-derived gene sets identified a cluster of genes involved in ubiquitylation and protein degradation (Fig. 4C). Although we failed to identify a specific new degradation pathway involving ΔNp63, this result suggests that wild-type ΔNp63α, but not the transcriptionally inactive mutants, might be involved in a feedback loop controlling its own stability, perhaps by upregulating an as-yet unknown ubiquitin E3 ligase or an accessory factor. Recent studies have identified IRF6 as a new regulator for p63 protein stability in mice palate development and keratinocytes (Moretti et al., 2010; Thomason et al., 2010). However, the investigators failed to identify the molecular mechanism by which IRF6, being a transcription factor, contribute to proteasome-mediated p63 degradation. In the above cited studies, the authors investigated exclusively one transcriptionally inactive mutant (the EEC mutants, R279H) that was resistant to IRF6-mediated downregulation. Our data clearly indicate that, besides IRF6, a new direct mechanism dependent on p63 transcription activity could contribute to the control of ΔNp63 stability.

The DBD and SAM domain mutants, but not those in the C-terminus, in general show absent or drastically reduced transcriptional activity. This is not due to altered localization because all the mutants tested exhibited normal nuclear staining. Moreover, all the mutants tested showed normal DNA binding, as assessed by ChIP. In addition to their greatly reduced transcriptional activity on promoters of genes such as K14 and BPAG-1, the DBD and SAM domain mutants can inhibit the transcriptional activity of wild-type ΔNp63α because they retained their capacity to form heteromeric p63 complexes. Because EEC and AEC are autosomal dominant disorders, the DBD and SAM mutations associated with these diseases have a dual effect on expression of epidermal proteins: by being transcriptionally deficient themselves, and by inhibiting transactivation by the residual wild-type allele.

By contrast, the C-terminal mutants both retain transcriptional competence and fail to inhibit effectively transcription by wild-type ΔNp63α, perhaps explaining the lack of a skin phenotype in these patients. An extensive analysis of the Q634X mutant (Fig. 6) showed that it has different effects in driving the expression of different target genes transcripts. The effect of the Q634X mutant is likely due to misexpression of specific target genes during limb development.
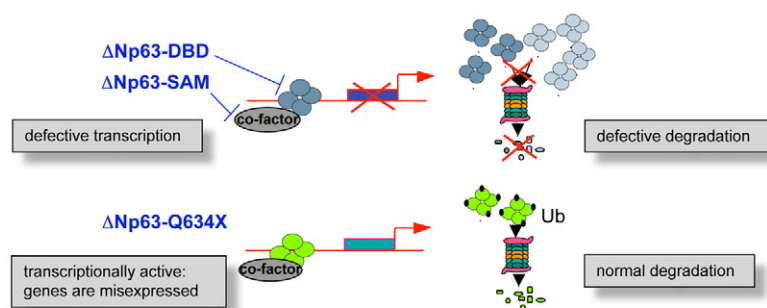
Fig. 7. Transcription and degradation are both involved in EDS pathogenesis. Differential molecular basis for distinct EDS are shown, highlighting the role of individual proteins domains. The model illustrates that wild-type and C-terminal mutants, which are transcriptionally active, are normally degraded via proteosoma. The DBD mutants and the SAM mutants, transcriptionally inactive, accumulate in the cells. This suggests the existence of a regulatory loop in which p63 degradation depends on the transactivation of one or more p63 target genes directly (as shown in the scheme) or indirectly (affecting the degradation machinery). By contrast, the transcriptionally active Q634X mutant degrades normally. We therefore hypothesize that the effects of the Q634X mutants are probably due to defective expression of specific target genes during limb development.

   Taken together, our results highlight the fact that both transcription and degradation are involved in EDS pathogenesis. Here, we provide a differential molecular basis for distinct EDS, highlighting the role on individual protein domains and contributing to an understanding of the molecular basis for the observed genotype–phenotype relationships (Fig. 7). Additional environmental and/or epistatic effects are likely to be superimposed on these basic molecular pathologies, and to account for inter-patient variation in disease expression.

Materials and Methods

Cell culture, plasmids and transfection
H1299 were grown in RPMI medium (GibcoBRL), and HEK293T were grown in Dulbecco's modified Eagle's medium (GibcoBRL). All media were supplemented with 10% (vol/vol) fetal bovine serum (GibcoBRL), and cells were cultured at 37°C in a humidified atmosphere of 5% (vol/vol) CO_2 in air. N-terminally Myc-tagged Itch plasmids and N-terminally FLAG-tagged TAp63α and ΔNp63α constructs were as described previously (Rossi et al., 2006). EDS-related p63 mutants were generated from pcDNA3 plasmids containing human N-terminally HA-tagged wild-type TAp63α or ΔNp63α using the QuikChange site-directed mutagenesis kit (Stratagene). Co-transfected GFP-expressing plasmid pEGFP-C1 was used to confirm efficient transfection in all experiments. Where required, empty pcDNA3-HA, FLAG or Myc vector was added to ensure equal total amounts of plasmid DNA in each transfection. Transient transfections were performed with Lipofectamine 2000 reagent according to the protocol of the manufacturer (Invitrogen).

Western blot and antibodies
Western blots were performed following standard procedures, using polyvinylidene fluoride membranes (PVDF). Detection was performed with the Amersham ECL Western Blotting Detection System (GE Healthcare). Endogenous Itch was detected with mouse monoclonal antibody (BD Biosciences), actin was detected with C-11 goat polyclonal antibody (Santa Cruz Biotechnology), GFP was detected with 33-2600 mouse monoclonal antibody (Invitrogen), p63 was detected with 4A4 monoclonal mouse antibody (Santa Cruz Biotechnology), the HA-tagged constructs were detected or immunoprecipitated with the HA-7 monoclonal mouse antibody (Sigma), the c-Myc-tagged constructs were detected or immunoprecipitated with the 9B11 monoclonal mouse antibody (Cell Signaling Technology), and the Flag-tagged constructs were detected or immunoprecipitated with the M2 monoclonal mouse antibody (Sigma).

Human primary keratinocyte culture
Skin biopsies from the trunk were taken from EEC patients carrying R204W, R279H, R280C and R304W mutations and from AEC patients with T533P and G561D mutations to establish the primary keratinocyte culture. Keratinocyte culture in Keratinocyte GroWTh medium (KGM) was as previously described (Rinne et al., 2008). Differentiation of keratinocytes was initiated by removing the GroWTh factors in KGM when cells were fully confluent.

Immunoprecipitation
Cells were transiently transfected with the indicated mammalian expression plasmids and harvested 48 hours after transfection. Cells were lysed on ice in a solution containing 50 mM Tris-HCl (pH 8.0), 150 mM NaCl, 1 mM EGTA (pH 8.0), 100 mM NaF (pH 8.0), 10% glycerol, 1 mM $MgCl_2$, 1 mM sodium orthovanadate, 1% (vol/vol) Triton X-100, and complete protease inhibitors (Roche). Protein concentrations were determined with the Bio-Rad protein assay reagent. Immunoprecipitation were performed by incubating 1.5 mg of whole-cell extracts with the indicated antibodies pre-bound to Protein-G Agarose beads (KPL, Gaithersburg, MD) and mixing gently for 1 hour at 4°C. Immunoprecipitates were then washed four times in lysis buffer and denatured in reducing Laemmli buffer. For alkaline phosphatase treatment, immunoprecipitates were washed four times with PBS then resuspended in 50 ml buffer, plus 10 units calf intestinal alkaline phosphatase (New England Biolabs) in the absence or presence of phosphatase inhibitors (10 mM $NaVO_4$ and 50 mM EDTA) and incubated for 60 minutes at 37°C. For co-immunoprecipitation showing the binding of Itch to different DNp63 mutants (supplementary material Fig. S2), the cells treated for 40 minutes with or without proteasome inhibitor MG132, at a final concentration of 50 μM in DMSO.

Steady-state protein level analysis
Levels of p63 proteins were determined 48 hours after co-transfection with the indicated combination of plasmids. Cell lysates were subjected to western blotting. p63 proteins were detected by using an anti-HA antibody. The same blots were re-probed with anti-Myc antibody to detect Itch. Anti-actin antibody was used as a loading control and anti-GFP as a control for efficient transfection. ^{35}S pulse-chase experiments were performed as described previously (Rossi et al., 2006).

Chromatin immunoprecipitation and luciferase reporter assays
Chromatin immunoprecipitation to access binding to the first, second and third p53 responsive site in the K14 promoter was carried out as previously described (Candi et al., 2006) in Saos 2 cell lines stably expressing the indicated wild-type or SAM domain point mutants of ΔNp63α and TAp63α proteins. The following primers amplifying the main p53 responsive element in the K14 promoter were used: forward 5′-CCTCTTCGGCCGGTGGAC-3′ and reverse 5′-CCGTTTTCGACCCTGAGAG-3′. Luciferase reporter assays for transactivational activity were carried out in HEK 293 cells as previously described (Candi et al., 2006) using the firefly luciferase gene under the control of the K14, EVPL, BPAG-1 promoter and expression vectors encoding for wild-type or mutant TAp63α and ΔNp63α.

Immunofluorescence and confocal analysis of skin biopsies
Skin biopsies from patients and unaffected individuals were obtained from informed volunteers according to hospital ethical committee practice and fixed in 4% buffered formaldehyde solution. Tissue samples were then stained for p63, K14, K10 and Ki67, and counterstained for DNA (DAPI) as described previously (Candi et al., 2006). Slides were analyzed with a confocal laser microscope (LSM 510; Zeiss). Quantification of the signal was performed using Laboratory Imaging software (Nikon).

RNA extraction and quantitative real-time RT-PCR
Total RNA was extracted by by using the RNAeasy kit (Qiagen, Milan, Italy) and quantified by spectrophotometric analysis. Total RNA (500 ng) was used for reverse transcription using the InPromII kit (Promega, Madison, WI) following the manufacturer's instructions. Real-time PCR was performed using Platinum SYBR Green qPCR SuperMix UDG (Invitrogen), with the following amplification file: one cycle of 3 minutes at 95°C, and 40 cycles of 20 seconds at 94°C and 40 seconds at 59°C. PCR reaction was followed by a melting curve protocol according to the specification of the ABI 7500 instrument (Applied Biosystems). Human β-actin mRNA was used as housekeeping gene for quantity normalization. Relative quantification of gene expression was calculated according to the method of $2^{-\Delta\Delta Ct}$ described in ABI User Bulletin no. 2 (http://www3.appliedbiosystems.com/cms/groups/mcb_support/ documents/generaldocuments/cms_040980.pdf, updated on October 2001) and the RQ software version 1.3 of Applied Biosystems. Primer pairs used in PCR reactions are: PERP forward 5′-TGTGGTGGAAATGCTCCCAAG-3′, PERP reverse 5′-CCAATCACTCTCAGGAAGACAAGC-3′; MTUS1 forward 5′-TTCCACG-GAGCAGGCTGTTC-3′, MTUS1 reverse 5′-AAGGGATGGCGGAGGATGTG-3′; p21 forward 5′-TGGGGATGTCCGTCAGAAC-3′, p21 reverse 5′-GGCGTTTG-GAGTGGTAGAAATC-3′; CycD1 forward 5′-AGAGGCGGAGGAGAACAA-ACAG-3′, CycD1 reverse 5′-AGGCGGTAGTAGGAC AGGAAGTTG-3′; DLL1 forward 5′-CCCAGAGGACAGAAGTGGATTG-3′, DLL1 reverse 5′-CC-GATAGTGGATAAACACAGCCTG-3′; PROX1 forward 5′-GAGCCTCCGTG-GAACTCA-3′, PROX1 reverse 5′-TGGGCACAGCTCAAGAATC-3′; DSP forward 5′-TGGAACCTGCCAAGATGTCAAC, DSP reverse 5′-TGATGTGGTGAGAA-GACCCCTG-3′; K17-forward 5′-TCAATGTGGAGATGGACGCTG-3′, K17-reverse 5′-TGCTGAAGAACCAATCCTCGGC-3′; β-act forward 5′-CTGGCACCA-CACCTTCTACAATG-3′, β-act reverse 5′-TAGCACAGCCTGGATAGCAAC-3′.

Gene array
Affymetrix gene expression microarrays were analyzed using Affymetrix proprietary software for image processing. The rma algorithm (Bolstad et al., 2003), as implemented in the 'affy' Bioconductor package (Gautier et al., 2004), was used to generate normalized probe-set signals. Gene sets derived from Gene Ontology-based annotations were tested for enrichment in upregulated and downregulated genes (p63 versus control) using the GSEA algorithm (Gene-Set Enrichment Analysis) (Subramanian et al., 2005). Gene-set enrichment results were explored using the Cytoscape plugin Enrichment Map (Merico et al., 2010).

References
Bakkers, J., Camacho-Carvajal, M., Nowak, M., Kramer, C., Danger, B. and Hammerschmidt, M. (2005). Destabilization of DeltaNp63alpha by Nedd4-mediated ubiquitination and Ubc9-mediated sumoylation, and its implications on dorsoventral patterning of the zebrafish embryo. *Cell Cycle* **4**, 790-800.
Bolstad, B. M., Irizarry, R. A., Astrand, M. and Speed, T. P. (2003). A comparison of normalization methods for high density oligonucleotide array data based on variance and bias. *Bioinformatics* **19**, 185-193.
Candi, E., Rufini, A., Terrinoni, A., Dinsdale, D., Ranalli, M., Paradisi, A., De Laurenzi, V., Spagnoli, L. G., Catani, M. V., Ramadan, S. et al. (2006). Differential

roles of p63 isoforms in epidermal development: selective genetic complementation in p63 null mice. *Cell Death Differ.* **13**, 1037-1047.

Candi, E., Dinsdale, D., Rufini, A., Salomoni, P., Knight, R. A., Mueller, M., Krammer, P. H. and Melino, G. (2007a). TAp63 and DeltaNp63 in cancer and epidermal development. *Cell Cycle* **6**, 274-285.

Candi, E., Rufini, A., Terrinoni, A., Giamboi-Miraglia, A., Lena, A. M., Mantovani, R., Knight, R. and Melino, G. (2007b). DeltaNp63 regulates thymic development through enhanced expression of FgfR2 and Jag2. *Proc. Natl. Acad. Sci. USA* **104**, 11999-12004.

Carroll, D. K., Carroll, J. S., Leong, C. O., Cheng, F., Brown, M., Mills, A. A., Brugge, J. S. and Ellisen, L. W. (2006). p63 regulates an adhesion programme and cell survival in epithelial cells. *Nat. Cell Biol.* **8**, 551-561.

Celli, J., Duijf, P., Hamel, B. C., Bamshad, M., Kramer, B., Smits, A. P., Newbury-Ecob, R., Hennekam, R. C., Van Buggenhout, G., van Haeringen, A. et al. (1999). Heterozygous germline mutations in the p53 homolog p63 are the cause of EEC syndrome. *Cell* **99**, 143-153.

Cicero, D. O., Falconi, M., Candi, E., Mele, S., Cadot, B., Di Venere, A., Rufini, S., Melino, G. and Desideri, A. (2006). NMR structure of the p63 SAM domain and dynamical properties of G534V and T537P pathological mutants, identified in the AEC syndrome. *Cell Biochem. Biophys.* **44**, 475-489.

Dohn, M., Zhang, S. and Chen, X. (2001). p63alpha and DeltaNp63alpha can induce cell cycle arrest and apoptosis and differentially regulate p53 target genes. *Oncogene* **20**, 3193-3205.

Duijf, P. H., Vanmolkot, K. R., Propping, P., Friedl, W., Krieger, E., McKeon, F., Dotsch, V., Brunner, H. G. and van Bokhoven, H. (2002). Gain-of-function mutation in ADULT syndrome reveals the presence of a second transactivation domain in p63. *Hum. Mol. Genet.* **11**, 799-804.

Ellisen, L. W., Ramsayer, K. D., Johannessen, C. M., Yang, A., Beppu, H., Minda, K., Oliner, J. D., McKeon, F. and Haber, D. A. (2002). REDD1, a developmentally regulated transcriptional target of p63 and p53, links p63 to regulation of reactive oxygen species. *Mol. Cell* **10**, 995-1005.

Fomenkov, A., Huang, Y. P., Topaloglu, O., Brechman, A., Osada, M., Fomenkova, T., Yuriditsky, E., Trink, B., Sidransky, D. and Ratovitski, E. (2003). P63 alpha mutations lead to aberrant splicing of keratinocyte growth factor receptor in the Hay-Wells syndrome. *J. Biol. Chem.* **278**, 23906-23914.

Gautier, L., Cope, L., Bolstad, B. M. and Irizarry, R. A. (2004). affy-analysis of Affymetrix GeneChip data at the probe level. *Bioinformatics* **20**, 307-315.

Ghioni, P., D'Alessandra, Y., Mansueto, G., Jaffray, E., Hay, R. T., La Mantia, G. and Guerrini, L. (2005). The protein stability and transcriptional activity of p63alpha are regulated by SUMO-1 conjugation. *Cell Cycle* **4**, 183-190.

Gu, X., Lundqvist, E. N., Coates, P. J., Thurfjell, N., Wettersand, E. and Nylander, K. (2006). Dysregulation of TAp63 mRNA and protein levels in psoriasis. *J. Invest. Dermatol.* **126**, 137-141.

Huang, Y. P., Wu, G., Guo, Z., Osada, M., Fomenkov, T., Park, H. L., Trink, B., Sidransky, D., Fomenkov, A. and Ratovitski, E. A. (2004). Altered sumoylation of p63alpha contributes to the split-hand/foot malformation phenotype. *Cell Cycle* **3**, 1587-1596.

Huang, Y. P., Kim, Y., Li, Z., Fomenkov, T., Fomenkov, A. and Ratovitski, E. A. (2005). AEC-associated p63 mutations lead to alternative splicing/protein stabilization of p63 and modulation of Notch signaling. *Cell Cycle* **4**, 1440-1447.

Laurikkala, J., Mikkola, M. L., James, M., Tummers, M., Mills, A. A. and Thesleff, I. (2006). p63 regulates multiple signalling pathways required for ectodermal organogenesis and differentiation. *Development* **133**, 1553-1563.

Lena, A. M., Shalom-Feuerstein, R., di Val Cervo, P. R., Aberdam, D., Knight, R. A., Melino, G. and Candi, E. (2008). miR-203 represses 'stemness' by repressing DeltaNp63. *Cell Death Differ.* **15**, 1187-1195.

Lo Iacono, N., Mantero, S., Chiarelli, A., Garcia, E., Mills, A. A., Morasso, M. I., Costanzo, A., Levi, G., Guerrini, L. and Merlo, G. R. (2008). Regulation of Dlx5 and Dlx6 gene expression by p63 is involved in EEC and SHFM congenital limb defects. *Development* **135**, 1377-1388.

McGrath, J. A., Duijf, P. H., Doetsch, V., Irvine, A. D., de Waal, R., Vanmolkot, K. R., Wessagowit, V., Kelly, A., Atherton, D. J., Griffiths, W. A. et al. (2001). Hay-Wells syndrome is caused by heterozygous missense mutations in the SAM domain of p63. *Hum. Mol. Genet.* **10**, 221-229.

Merico, D., Isserlin, R., Stueker, O., Emili, A. and Bader, G. D. (2010). Enrichment map: a network-based method for gene-set enrichment visualization and interpretation. *PLoS ONE* **5**, e13984.

Mills, A. A., Zheng, B., Wang, X. J., Vogel, H., Roop, D. R. and Bradley, A. (1999). p63 is a p53 homologue required for limb and epidermal morphogenesis. *Nature* **398**, 708-713.

Moretti, F., Marinari, B., Lo Iacono, N., Botti, E., Giunta, A., Spallone, G., Garaffo, G., Vernersson-Lindahl, E., Merlo, G., Mills, A. A. et al. (2010). A regulatory feedback loop involving p63 and IRF6 links the pathogenesis of 2 genetically different human ectodermal dysplasias. *J. Clin. Invest.* **120**, 1570-1577.

Pozzi, S., Zambelli, F., Merico, D., Pavesi, G., Robert, A., Maltere, P., Gidrol, X., Mantovani, R. and Vigano, M. A. (2009). Transcriptional network of p63 in human keratinocytes. *PLoS ONE* **4**, e5008.

Radoja, N., Guerrini, L., Lo Iacono, N., Merlo, G. R., Costanzo, A., Weinberg, W. C., La Mantia, G., Calabro, V. and Morasso, M. I. (2007). Homeobox gene Dlx3 is regulated by p63 during ectoderm development: relevance in the pathogenesis of ectodermal dysplasias. *Development* **134**, 13-18.

Rinne, T., Hamel, B., van Bokhoven, H. and Brunner, H. G. (2006a). Pattern of p63 mutations and their phenotypes-update. *Am. J. Med. Genet. A* **140**, 1396-1406.

Rinne, T., Spadoni, E., Kjaer, K. W., Danesino, C., Larizza, D., Kock, M., Huoponen, K., Savontaus, M. L., Aaltonen, M., Duijf, P. et al. (2006b). Delineation of the ADULT syndrome phenotype due to arginine 298 mutations of the p63 gene. *Eur. J. Hum. Genet.* **14**, 904-910.

Rinne, T., Brunner, H. G. and van Bokhoven, H. (2007). p63-associated disorders. *Cell Cycle* **6**, 262-268.

Rinne, T., Clements, S. E., Lamme, E., Duijf, P. H., Bolat, E., Meijer, R., Scheffer, H., Rosser, E., Tan, T. Y., McGrath, J. A. et al. (2008). A novel translation re-initiation mechanism for the p63 gene revealed by amino-terminal truncating mutations in Rapp-Hodgkin/Hay-Wells like syndromes. *Hum. Mol. Genet.* **17**, 1968-1977.

Rossi, M., Aqeilan, R. I., Neale, M., Candi, E., Salomoni, P., Knight, R. A., Croce, C. M. and Melino, G. (2006). The E3 ubiquitin ligase Itch controls the protein stability of p63. *Proc. Natl. Acad. Sci. USA* **103**, 12753-12758.

Senoo, M., Pinto, F., Crum, C. P. and McKeon, F. (2007). p63 Is essential for the proliferative potential of stem cells in stratified epithelia. *Cell* **129**, 523-536.

Serber, Z., Lai, H. C., Yang, A., Ou, H. D., Sigal, M. S., Kelly, A. E., Darimont, B. D., Duijf, P. H., Van Bokhoven, H., McKeon, F. et al. (2002). A C-terminal inhibitory domain controls the activity of p63 by an intramolecular mechanism. *Mol. Cell. Biol.* **22**, 8601-8611.

Subramanian, A., Tamayo, P., Mootha, V. K., Mukherjee, S., Ebert, B. L., Gillette, M. A., Paulovich, A., Pomeroy, S. L., Golub, T. R., Lander, E. S. et al. (2005). Gene set enrichment analysis: a knowledge-based approach for interpreting genome-wide expression profiles. *Proc. Natl. Acad. Sci. USA* **102**, 15545-15550.

Thomason, H. A., Zhou, H., Kouwenhoven, E. N., Dotto, G. P., Restivo, G., Nguyen, B. C., Little, H., Dixon, M. J., van Bokhoven, H. and Dixon, J. (2010). Cooperation between the transcription factors p63 and IRF6 is essential to prevent cleft palate in mice. *J. Clin. Invest.* **120**, 1561-1569.

Vigano, M. A., Lamartine, J., Testoni, B., Merico, D., Alotto, D., Castagnoli, C., Robert, A., Candi, E., Melino, G., Gidrol, X. et al. (2006). New p63 targets in keratinocytes identified by a genome-wide approach. *EMBO J.* **25**, 5105-5116.

Westfall, M. D., Mays, D. J., Sniezek, J. C. and Pietenpol, J. A. (2003). The Delta Np63 alpha phosphoprotein binds the p21 and 14-3-3 sigma promoters in vivo and has transcriptional repressor activity that is reduced by Hay-Wells syndrome-derived mutations. *Mol. Cell. Biol.* **23**, 2264-2276.

Yang, A., Kaghad, M., Wang, Y., Gillett, E., Fleming, M. D., Dotsch, V., Andrews, N. C., Caput, D. and McKeon, F. (1998). p63, a p53 homolog at 3q27-29, encodes multiple products with transactivating, death-inducing, and dominant-negative activities. *Mol. Cell* **2**, 305-316.

Yang, A., Schweitzer, R., Sun, D., Kaghad, M., Walker, N., Bronson, R. T., Tabin, C., Sharpe, A., Caput, D., Crum, C. et al. (1999). p63 is essential for regenerative proliferation in limb, craniofacial and epithelial development. *Nature* **398**, 714-718.

Yang, A., Zhu, Z., Kapranov, P., McKeon, F., Church, G. M., Gingeras, T. R. and Struhl, K. (2006). Relationships between p63 binding, DNA sequence, transcription activity, and biological function in human cells. *Mol. Cell* **24**, 593-602.

Yi, R., Poy, M. N., Stoffel, M. and Fuchs, E. (2008). A skin microRNA promotes differentiation by repressing 'stemness'. *Nature* **452**, 225-229.